Volcano monitor using broadcast satellite signals

*Hiroshi Takiguchi[1], Tadahiro Gotoh[1], Masatake Harada[2], Jun Amagai[1], Mikio Satomura[2]

1.Applied Electromagnetic Research Institute, National Institute of Information and Communications Technology, 2.Hot Springs Research Institute of Kanazawa Prefecture

We cannot see the change of an internal active volcano condition directly by its geography then, perceiving of its activities is difficult. To mitigate disasters by eruption, continuous volcano activity monitoring system will be desired. Most active volcanoes radiate internal thermal energy as a water vapor, and this radiation is increase with increasingly active volcano. The propagation speed of electromagnetic signal in the neutral atmosphere is delayed by the change of refractivity, which is a function its temperature, pressure, and water vapor. Therefore, to measure the propagation delay changes on volcano crater may be possible to estimate the vitalization of active volcano. We have devised a volcano activity monitor using broadcast satellite signals. In this presentation, we describe the details of the system, and show the result of feasibility survey at Hakone.

Keywords: volcano, VLBI, broadcast satellite

FEM modeling and GNSS observation around Mount Ontake volcan

*Takeo Ito[1], Kenjiro Matsuhiro[1]

1.Earthquake and Volcano Research Center, Graduate School of Environmental Studies, Nagoya University

On Septmber 27, 2014, Mount Ontake volcano was erupt. The eruption took 63 lives and represented the worst volcanic disaster in post-World War II Japanese history. Before this eruption, the GNSS observations are a few around Mount Ontake volcano. Especially, the number of GNSS observation within 4km from the summit of mount Ontake volcano is only one, which is belong to JMA. After the eruption, we establish GNSS observation network around mount Ontake volcano. New GNSS observation network around mount Ontake volcano are consistent of six continues GNSS sites. Two and four continues GNSS sites stared at 2014 and 2015, respectively. We also make seven campaign GNSS sites where are located at eastern side of mount Ontake volcano. These campaign GNSS sites are observed at July 2015.
In order to explain the observed crustal deformation, we make FEM model considering topography, such as shape of the mount Ontake volcano. In this poster, we introduce the new GNSS observation and FEM model for mount Ontake volcano.

Keywords: GNSS, Mount Ontake volcano, FEM

Characteristics of tilt changes during eruption at Sakurajima: analysis of tilt data at Amidagawa station, Japan Meteorological Agency (JMA)

*Ryosuke Nakajima[1], Takeshi Nishimura[1]

1.Department of Geophysics, Graduate School of Science,Tohoku University

Tilt change records have been used to clarify the source mechanism of volcanic eruptions and magma processes beneath the volcanoes. This study give focuses on the characteristic behaviors in temporal tilt changes during eruptions and its relations to the extrusion volume.
This study uses NS component of tilt data at Amidagawa station, which is installed 3 km away from the Syowa crater, because the data clearly records the clear tilt changes accompanied with each explosion. After eliminating tidal components in the observed tilt record using Baytap08 (Tamura et al.,2013), we selected explosive eruptions whose plume height is higher than 2000m in April and May of 2015, based on the explosion list by Kagoshima Meteorological Office. We further chose 24 eruptions in which uplift and subsidence of the crater directions are clearly observed.
In all of the events, we can see the following characteristics in tilt changes; tilt uplift rapidly toward the crater 1~2 minutes before the explosion; the uplift continues for a while, and turns to subsidence tens of seconds to a few minutes after the onset of explosion. Uplift tilt change toward the crater just after the explosion suggests that vertical upward force affect inside the conduit accompanying ash extrusion, and subsidence can be considered to represent deflation of conduit and magma chamber due to magma extrusion. Amount of tilt change of uplift, subsidence were from 2nrad to 10nrad, from 2.5nrad to 37nrad, respectively. Similarly, duration of them were from 1minute to 3.5minutes, from 10minutes to 140 minutes.
We do not see clear correlations between amount of tilt change, duration and plume height, column volume. Then, we give a focus on the amount of tilt change per unit time (tilt rate), and we find the tilt changes are classified into 2 type of subsidence; one subside rapidly within 10 minutes (Type A), and another subside gradually (Type B). Relations between tilt rate just after the start of deflation, plume height, column volume show positive correlations especially for Type A. Similar results are obtained for the uplift tilt rate.

Keywords: Tilt, Plume height, Sakurajima, Explosion

Relationship between eruption plume heights and seismic source amplitudes estimated of eruption tremors and explosion events

*azusa mori[1], Hiroyuki Kumagai[1]

1.Nagoya University Environmental Studies

It is important to analyze and interpret tremors and volcanic earthquakes for estimating eruption size and for understanding eruption phenomena. In this study, we focus on eruption tremors and explosion events to understand physical processes of eruptions and to contribute to realtime estimation of eruption size.
Previous studies investigated the relation between eruption tremor and eruption size. McNutt (2004) studied the relation between the reduced displacement (DR) of tremor and the volcano explosivity index (VEI). However, there is a wide range of DR values for each VEI, so that VEI could be overestimated or underestimated from DR. Furthermore, there are the following problems in DR: (1) The estimated DR depends on tremor's frequency, and (2) the duration of tremor is not taken into account.
Kumagai et al. (2015) estimated the source amplitudes (As) and cumulative source amplitudes (Is) for eruption tremors and explosion events at Tungurahua, Ecuador, using the amplitude source location (ASL) method based on the assumption of isotropic S-wave radiation in a high-frequency band (5-10 Hz). Their results indicated that (1) Is linearly increased with increasing As for explosion events, and (2) the log of Is was proportional to As for eruption tremors. However, the universality of these scaling relations is not confirmed yet, and the physical meanings of As and Is are also not clear.
In this study, we analyzed eruption tremors and explosion events observed at Japanese volcanoes to investigate the relations between As and Is. We used continuous seismic waveform data of Japan Meteorological Agency's volcano observation networks, which are available through the V-net website of the National Research Institute for Earth Science and Disaster Prevention (NIED). We analyzed eruption tremors and explosion events at Sakurajima (Aug. 2013-Sep.2015), Kuchinoerabu (May. 29, 2015), and Ontake (Sep. 27, 2014), for which we applied a band-pass filter of 5-10 Hz to obtain envelope waveforms. We assumed sources at vents and estimated As and Is using the ASL method. Then, we examined the relation between As and Is as well as As and the maximum heights of eruption plumes.
We obtained the linear relationship between As and Is for explosion events at the Japanese volcanoes, and these values were similar to those estimated at Tungurahua by Kumagai et al. (2015). This suggests that the linear relationship between As and Is for explosion events is universally held. Our comparison between As and maximum plume heights indicated that there is a linear relationship between them, suggesting that the plume height may be estimated from As. Is may be related to eruption volume, but it was not confirmed due to the lack of eruption volume data. Assuming the linear relationships between Is and eruption volume and between As and plume height and using the relation that the log of Is is proportional to As, we obtained the relationship that the log of eruption volume is proportional to the plume height. We compared this relation with that estimated by Mastine et al. (2009) for various eruptions in the world. We found that the proportionality coefficient between As and plume height estimated from this comparison and that estimated from the above analysis were very similar. This supports that the proportional relationship between As and plume height is widely held. However, the differences in eruption styles (vulcanian and plinian) must be taken into account in our interpretations of As and Is and their relations with the plume height and eruption volume, which are open to future studies.

The influence of the downwind on the stratigraphic GSD variation in the 2D fall and sedimentation model

*Yu Iriyama[1], Atsushi Toramaru[2]

1.Department of Earth and Planetary Sciences, Graduate School of Sciences, Kyushu University,
2.Department of Earth and Planetary Sciences, Faculty of Science, Kyushu University

The stratigraphic variation of grain-size distribution (GSD) in pyroclastic fall deposit indicates the temporal variation of GSD of settling particles, and may reflect the temporal variation of the eruption. The temporal variation of eruption, especially the temporal variation of the source GSD, affect the temporal and spatial variations of GSD in the umbrella cloud. In order to relate the stratigraphic variation of GSD to the temporal variation of source GSD, it is necessary to take into account the fractionation process from the umbrella cloud and the transportation process of ejected particles.
We developed two-dimensional fall and sedimentation (2DFS) model in order to relate the temporal variations of GSDs between the source and the sediment. Our model deals with the influence of the fractionation from an umbrella cloud and the advective transportation caused by the downwind on the sediment GSD. In this study, we assess the influence of the downwind velocity on the sediment GSD and thickness as functions of stratigraphic height and distance from the source vent by numerically calculating the analytical representation.
As a result, in the same particle size at the same distance from the source vent, the number of particles of sediment in the 2DFS model with downwind is larger than that one without downwind due to the effective shortening of fractionation times. This difference in the particle number affects the thickness of sediment. Similarly, travel time of particles, which settle at a certain distance from the source vent, with downwind is shorter than that one without downwind.
Without downwind, the order of settling particles is from the largest particles to the finer particles resulting in the normal grading structure. However, with downwind, it is possible to settle from the finer particles than the largest particles due to the dominancy of advective lateral transportation by downwind rather than by sedimentation with size sorting. This suggests that the reverse grading structure of the pyroclastic fall deposit may result from the downwind effect.

Keywords: pyroclastic fall deposit, stratigraphic variation, temporal variation of explosive eruption, effects of downwind, reverse grading structure

Changing timescale from magma mixing to ejection with eruptive timing-An example from the Shinmoe-dake 2011 eruption-

*Yuki Suzuki[1], Takeyoshi Sakai[1], Mie Ichihara[2]

1.Department of Earth Sciences, Faculty of Education and Integrated Arts of Sciences, Waseda University, 2.ERI, Univ. of Tokyo

Investigating mechanism and timescale of eruption triggering is one of the important tasks in volcanology. Injection of high temperature magma into the low temperature magma reservoir triggered the Shinmoe-dake 2011 eruption, by remobilizing the mush-like, immobile low temperature magma (Suzuki *et al.*, 2013). Some studies (Tomiya *et al.*, 2013; Suzuki *et al.*, 2013) already reported timescale from magma mixing to eruption for this eruption, by using zoning (diffusion) profiles in magnetite phenocrysts originated from the low temperature magma; that varies between 0.7h and 15.2h in Suzuki *et al.* (2013) which investigated several magnetite phenocrysts in a pumice clast erupted in the late stage of the second sub-Plinian (Jan 27AM) event. However, it remained unsolved whether timescale from magma mixing to eruption has correlation with eruption timing. If the timescale is constant throughout the 2011 eruption, it means magma mixing occurred repeatedly (e.g. Nakamura, 1995). We here focus on three sub-Plinian events (Jan 26PM, 27AM, 27PM) that occurred intermittently in the climactic phase of the 2011 eruption. To answer above question, we examined a succession of sub-Plinian deposit (Layer 2-5, Nakada *et al.*, 2013).
In this preliminary study, only Layer2-low, Layer3-low and Layer4-low (“low” means lower part of each unit) were investigated. According to Suzuki *et al.* (2014, JpGU meeting), Layer-2low and Layer-3low are from the first sub-Plinian event, and Layer-4 low is from the second sub-Plinian event. Magnetites included in ash size particles (500-1400μm) were investigated. Relatively large magnetites are preferable to read chemical and thermal history, and maximum size of magnetite phenocryst in thin sections of hand-size pumice reaches 300μm (Suzuki *et al.*, 2013). The ash particles (both pumice and free crystal) including large magnetite can be more than 500μm. The reason why we used ash size particles was to randomly pick up magnetites with various histories and mount them on single microscope slide. For EPMA analyses, we used magnetite whose rim is in contact with groundmass and whose 2D size is more than 150μm to minimize cut-section effect. To acquire zoning profiles, point analyses were carried out at 5μm intervals and 10μm intervals for marginal part (up to 20μm from rim) and inner part, respectively. Number of investigated magnetite reached ca. 20 for each eruptive unit.
Although shapes of zoning profiles have a variation for 20 crystals, all show reverse zoning in MgO. Maximum MgO contents in reversely zoned parts do no systematically change with eruptive unit, which is consistent with the continuous ejection of equally mixed magmas of the same endmember magmas (Suzuki *et al.*, 2013). We found two tendencies this time. First, most magnetites from Layer2-low have reversely zoned parts only in the marginal parts (e.g. up to 20μm from the rim), which differs from magnetites of other units. This might indicate timescale from mixing to eruption was mostly shorter in mixed magmas erupted as Layer2-low deposit. This could happen if major magma mixing occurred only in the beginning of the whole sub-Plinian activity. The second point is related to MgO contents of the unzoned inner parts. The MgO contents for 20 grains show bimodal distribution only in Layer2-low. In addition, minimum MgO contents for 20 magnetites seem lower in Layer2-low. This might show the different thermal and chemical history of the remobilized low temperature magmas depending on the stage of whole sub-Plinian activity. Additional analyses for other eruptive units (Layer2-up, Layer3-up, Layer4-up and Layer5) and calculation of absolute timescale from mixing to eruption are necessary to confirm above models.

Keywords: Eruption triggering, Shinmoe-dake, Mush-like felsic magma, Magma mixing, Magnetite, Diffusion profiles

A new technique to analyse unexposed melt inclusions in quartz

*Shumpei Yoshimura[1], Mitsuhiro Nakagawa[1]

1.Department of Earth and Planetary Sciences, Hokkaido University

We are trying to develop a new technique to analyse the volatile concentration of quartz-hosted rhyolitic melt inclusions using a micro-FTIR spectrometer without exposing the inclusions to the surface of a doubly-polished thin section. This method is similar to that of Nichols and Wysoczanski (2007) who established a technique to analyse unexposed basaltic melt inclusions in olivine phenocryst. We show the results of the feasibility examination of this technique as summarised below.
When an infrared beam transmits through both the quartz crystal and melt, the resultant spectrum (f) is considered to be the linear combination of the pure spectrum of quartz and melt: f=d(qz)*f(qz)+d(mi)*f(mi). Here, f(qz) and f(mi) represent the pure spectrum of quartz and melt per unit thickness, respectively. d(qz) and d(mi) are the effective thickness. d(qz) is calculated based on the absorbance of a quartz peak in the sample spectrum that is considered to be linearly proportional to the thickness. d(mi) is then obtained by subtracting d(qz) from the total thickness (d). Finally, the volatile concentration is estimated from d(mi) and absorbance of the volatile peaks.
The feasibility of this analytical method was examined as follows. Firstly, we analysed quartz thin sections with a micro-FTIR spectrometer to confirm that absorbance of quartz peaks, which exist in the range of 1500-2200 cm-1, is proportional to quartz thickness. The 1790 cm-1 peak was chosen as an indicator of d(qz), because this peak is free from interference with other peaks.
Secondly, we examined if the mixed spectrum of quartz and melt is the linear combination of pure spectrum of each material, by putting a thin section of obsidian on the section of quartz. We confirmed that the mixed spectrum was the linear combination, and the water content of obsidian was always calculated to a single value irrespective of the quartz/melt ratio.
Thirdly, we applied the method to a quartz-hosted melt inclusion from the Onikobe caldera super eruption. A large inclusion with 150 μm diameter was chosen for this purpose. The water content of this inclusion was determined to be 4.4 wt% by an FTIR analysis with a 10 μm beam. The same inclusion was then analysed with a thick beam with various diameter(<300μm). We observed that the resultant spectrum was not a linear combination: the water content was strongly dependent on the quartz/melt ratio. For example, the water content was calculated to be 2.3 wt% based on 3550 cm^{-1} peak when d(qz)/d =0.23. For the 4500 and 5250 cm^{-1} peaks, the water content was calculated to be 63 and 84 % of the true water content. We are now investigating why such a non-ideal behaviour was observed in melt inclusion analysis, though ideal linearity was confirmed in the quartz+obsidian superimposed sample.

Keywords: melt inclusion, quartz, FTIR

Laboratory experiments on the whole process of magma chamber solidification

*Daichi Takahashi[1], Ikuro Sumita[1]

1.Graduate school of Natural Science and Technology, Kanazawa University

How does the initially totally molten and thermally convecting magma chamber solidify ? How is the solidification process and solidification texture related ? There have been experimental (e.g., Brandeis & Marsh, *Nature*, 1989) and theoretical (e.g., Worster et al., *EPSL*, 1990) studies focusing on how the melt solidifies when it is cooled. These studies have showed a complex coupling between solidification and thermal, compositional convection, but detailed study on the whole process of solidification is still limited. Here we conduct laboratory experiments using a wax to model magma and study the whole process until complete solidification under different thermal boundary conditions.
We use a thin acrylic tank with a height 80 mm, width 80 mm and a thickness of 10 mm. We fill the tank with a wax (PEG 1000) which solidifies at 37 degrees C. We heat the tank from below using a heater at a temperature of 70 degrees C. The wax melts and thermal convection occurs. The Prandtl number of the liquid PEG is Pr = 700 and the Rayleigh number of thermal convection is $Ra=2.4\times10^{7}$. After a steady state convection is achieved, we turn off the heater and the wax solidifies. We record the cooling process using time-lapse photos and measure the temperature within the liquid and at the boundaries. We conducted experiments under the following 3 thermal boundary conditions : Case A (Cooled from above at a room temperature and insulated from below), Case B (Cooled from above by an ice water and insulated from below), Case C (Cooled from below at a room temperature and insulated from above). From these experiments, we find the following: (i) the time needed for the total solidification is the same for the 3 cases within 5 %, (ii) for cases A and B, convective pattern changed during cooling and transformed to a single upwelling at the center and two downwellings at the sides whereas for Case B, convective pattern remained unchanged during solidification and only changed immediately before total solidification, (iii) solidification texturing occurred with a pattern corresponding to the temperature field of the thermal convection immediately before the total solidification.
Our experimental results can be interpreted as follows. (i) In our experiments the time required for total solidification is comparable regardless of the thermal boundary condition. When the boundary temperature is low, solidification occurs earlier, but suppresses the heat transfer thereafter due to the thickening thermal boundary layer. This seems to be the reason for the comparable total solidification time. (ii) In our experiments, in Case B, solidification started within a time scale shorter than the turnover time and the convection pattern remained unchanged. This is consistent with the estimate that at least a convective turnover time is needed for a convection pattern to change. (iii) Our experiments show solidification texturing corresponding to the temperature field of thermal convection immediately before solidification. The thermal diffusion time for the temperature field originating from thermal convection to become homogenized can be estimated as 4 hours, assuming a convection cell size of 4 cm. On the other hand, the time needed for total solidification after the convection stops is only about 15-18 min, which is much shorter than the thermal diffusion time, which explains why solidification texturing occurred. Our experiments suggest that similar phenomena may occur in magma chambers if the same conditions describe above are satisfied.

Keywords: magma chamber, solidification process, thermal convection, solidification texturing

Rheological experiments of polyurethane foam toward simulating tube pumice

*Masatoshi Ohashi[1], Mie Ichihara[1], Atsushi Toramaru[2], Osamu Kuwano[3]

1.The Earthquake Research Institute, the University of Tokyo, 2.Department of Earth and Planetary Sciences, Faculty of Sciences, 33 Kyushu University, 3.Japan Agency for Marine-Earth Science and Technology

Tube pumice is a common product of explosive silicic eruptions forming calderas. It is characterized by bubbles which elongate in one direction. Such bubble deformation is considered to occur in the processes of magma ascending in a conduit, which include vesiculation, flow, and fragmentation. It is expected that tube pumice has recorded information about some processes leading to a caldera eruption. In the preliminary experiment, we decompressed and inflated polyurethane foam (Ohashi et al., 2015, VSJ meeting). Polyurethane foam is a candidate of analogue materials to be used to simulate the formation processes of pumice because it undergoes vesiculation, flow, and solidification at ordinary temperature and pressure. Reproducing the tube pumice structure with polyurethane foam may help discovering the key factors to produce tube pumice. Here we present the time-dependent rheological properties of the polyurethane foam, which is specifically blended for our experiment.
Material : Polyurethane foam is a polymeric solid with a cellular structure. It is produced by mixing two polymeric liquids (polyisocyanate and polyol) with a catalyst and a foam stabilizer. Including a foam stabilizer prevents bubbles from coalescing and produces a homogeneous cellular structure by stabilizing their interfaces. To avoid such a structure, we use specifically blended polyurethane foam without the foam stabilizer in this study. This polyurethane foam has elliptical bubbles, which are larger than the usual one because of coalescing.
Apparatus and Procedure : We examine the temporal change of the rheology of the polyurethane foam from inflation to solidification. A rheometer (AR2000ex) is used with a concentric cylinder. The outer cylindrical cup is made of transparent polypropylene (inner φ=23 mm) and the rotating spindle is made of aluminum (outer φ=15 mm). An infrared thermometer is mounted at the side of the cup to record its temperature. The torque and the angle of the rotation are recorded by the rheometer and the growing height of the sample is measured in the video images. The data are used to calculate the stress and strain. In oscillatory tests, the amplitude ratio and the phase difference of the stress and the strain provide us with the storage modulus (G') representing elasticity and the loss modulus (G'') representing viscosity. We conduct three experiments. First, the temporal changes of G' and G'' are examined under oscillatory rotation with the frequency of 3.16 Hz and the strain amplitude of 0.1 %. Second, the frequency dependence is assessed by changing the frequency in a measuring cycle. Finally, a large strain is applied up to 10 at the strain rate of 0.2 (s^-1) while the material is solidifying. We look into the pore structure of the representative samples with X-ray tomographic imaging (inspeXio SMX-225CT, Shimadzu Co.).
Result and Discussion : In the initial stage G'' is larger than G' indicating the material is fluid. The torque gradually increases with the gelation, so that G' is equal to G'' in 20 minutes. After that, G'' decreases and G' converges into the constant value of $10^{6.3}$ Pa. It is known that the shear modulus of magma is about 10 GPa regardless of its temperature and composition (Dingwell and Webb, 1989). We find the shear modulus of the polyurethane foam used in this experiment is lower than that of magma by four orders. In the second experiment the crossing time when G' is equal to G'' is delayed as the frequency decreases. The inverse of the angular frequency at the crossing time is regarded as the instantaneous relaxation time. This result shows the relaxation time of the material gradually increases and the time scale in which the material transits from solid to liquid

is quantified. Finally the X-ray tomographic imaging reveals that the sample of the third experiment with a large strain has elongated bubbles like tubes.

Keywords: Polyurethane foam, Tube pumice, Rheology, X-ray tomographic imaging

Mechanism of fragmentation of vesicular magma with non-uniform distribution of bubbles

*Shogo Maruyama[1], Yamato Aoki[1], Noriaki Kurokawa[1], Hiroshi Yoshida[1], Masaharu Kameda[1], Mie Ichihara[2], Satoshi Okumura[3], Kentarou Uesugi[4]

1.Mech. Systems Eng.,TUAT, 2.ERI, Univ. of Tokyo, 3.Earth Sci., Tohoku Univ, 4.JASRI

Brittle fragmentation is a key process in explosive eruption. Estimation of the decompression time in real explosive events indicates that the style of fragmentation is to be “brittle-like fragmentation” (Kameda et al., JVGR 2013), which was defined as the solid-like fracture of the material whose bulk rheological properties was close to fluid state. In this presentation, we clearly show the internal non-uniform structure of bubbles which is a major source of crack development that may lead to brittle-like fragmentation. This scenario was proposed based on our previous experiments (Kameda et al., JGUM 2014).

We used syrup containing bubbles as material of specimen because syrup has large rigidity close to magma, and can have wide range of viscosity like magma. The rapid decompression apparatus was used to simulate the fragmentation. It consisted of a pressure container whose top was sealed by a plastic film. First we compressed the specimen placed in the container by nitrogen gas. Second we heated electrically the nichrome wire adhered on the film. The rapid decompression was caused by the rupture of the film due to the heat of nichrome wire.

The specimen was hemisphere whose size was about 20 mm in diameter and 10 mm in height. The viscosity of each specimen was chosen from three values (10, 50, and 100 MPa · s) and the void fraction before the decompressionφ_0 was varied from 4% to 40%. The initial pressure just before the decompression was 2 MPa, and the characteristic time of decompression was about 3 ms.

To observe the internal structure of specimen, we conducted X-ray CT imaging at SPring-8. We took the radiograph images with the resolution of 15.5 μm/pixel. The CT imaging was conducted three times (after and before the compression and after the decompression). We observed the dynamic behavior of specimen during decompression by radiography using the same optical setup as the CT imaging. We simultaneously observed it by high speed imaging using a visible light source. We reconstructed the volumetric 3D model of the specimen based on the CBP method.

A typical example of fragmentation captured by high speed imaging is shown in Fig. 1. This experiment was conducted under η=50 MPa · s,φ_0=7.6 %. As shown in Fig. 1, the partial fragmentation occurred at 2.1 ms after the decompression was started. Reconstructed 3D image of the specimen is shown Fig. 2. As shown in Fig. 2, the specimen contains a large bubble with a small satellite bubble close to the large one (green broken line). These two bubbles are triggers of the fragmentation shown in Fig. 1. We also observed all the specimen fragmented into pieces even if its viscosity was the same as that shown in Fig. 1. Therefore, it is concluded that whether to fragment or not depends on the bubble distribution.

Next, we conducted finite element analysis of the specimen under the rapid decompression. The COMSOL Multiphysics ver. 5.0 was used as calculation platform. In order to reduce computational cost, we used a simplified 3D model of the specimen in the experiment (Fig. 2). In the model, we extracted just around the primary large bubble with a satellite small bubble. The specimen was assumed to be a Maxwell fluid whose physical properties were equal to those of syrup measured in previous study.

As shown in the result (Fig. 3), the maximum stress occurred between the two bubbles. Preliminary result (Kurokawa et al. JGUM 2015) shows that the stress concentration occurs on the surface of satellite bubble, and it leads to the increase of brittleness (Ichihara et al. JGR 2010) at the time when the stress reaches the critical value of fracture. Compared the calculation result of

surface stress field with the surface crack distribution captured by high speed photography, we found that the surface crack propagates along the line of large stress concentration. This fact indicates that we can predict the brittle fracture.

Keywords: Magma, Fragmentation, X-ray CT, FEA

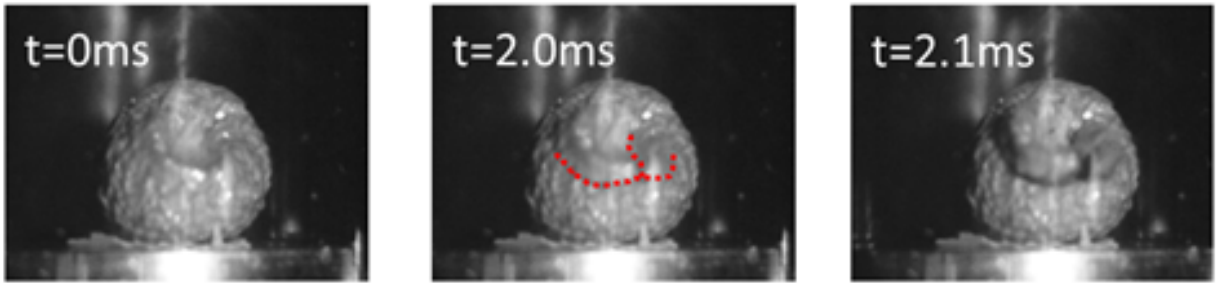

Fig.1 High-speed video images of fragmentation

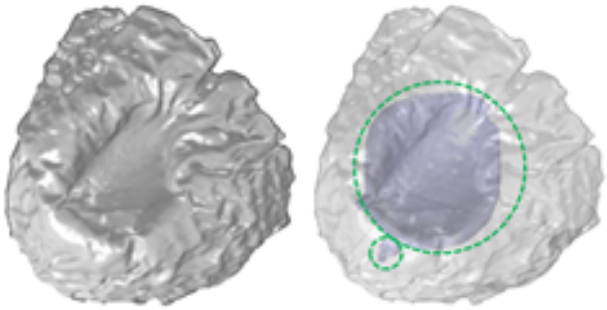

Fig.2 Surface and primary pores

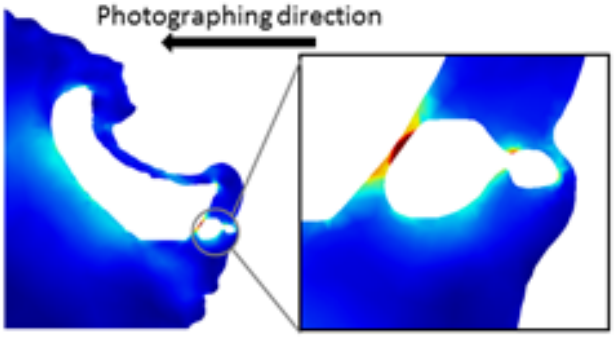

Fig.3 Stress at primary pores

